

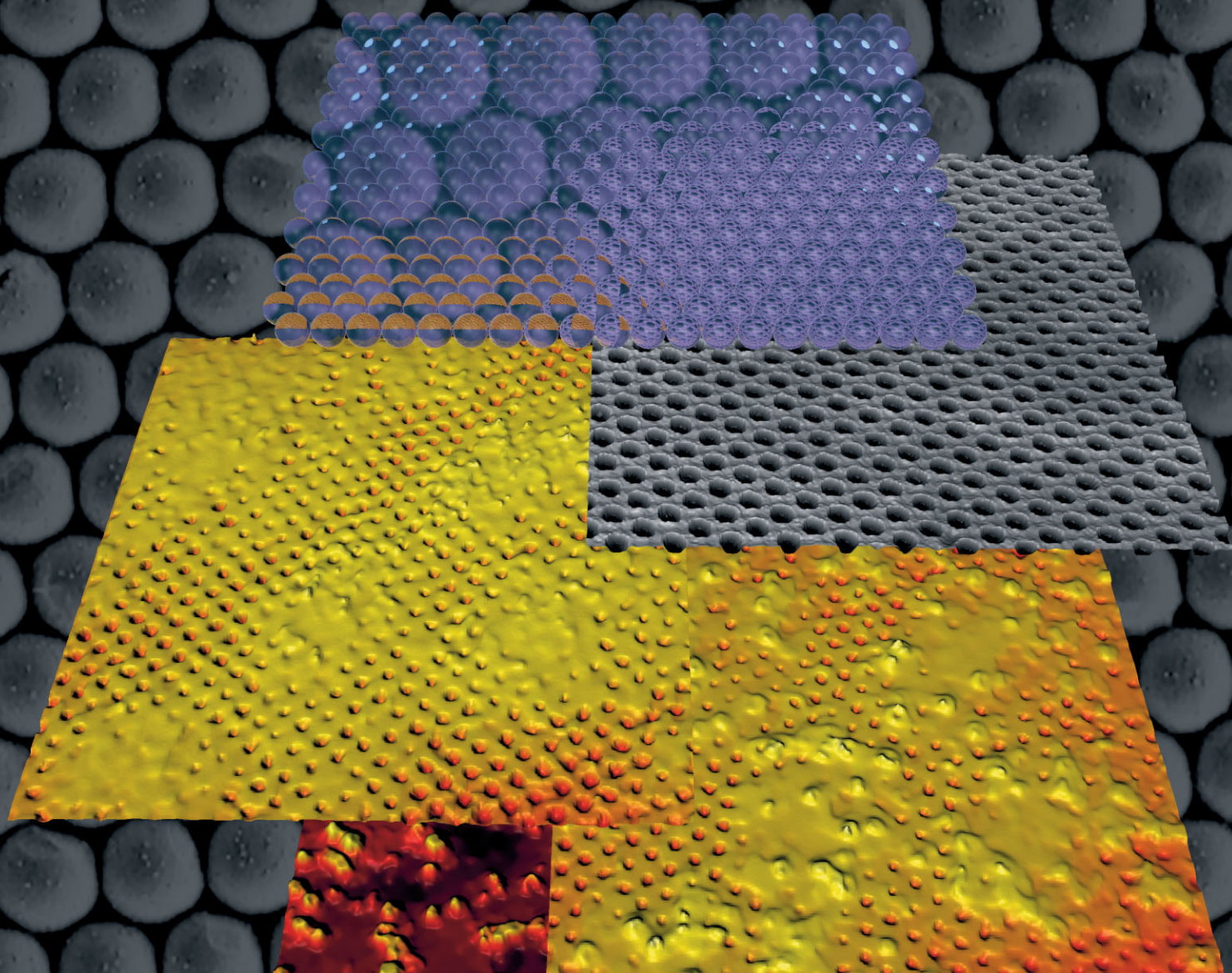
AFMDC6
ISSN 1616-301X
Vol. 17, No. 7
May 7, 2007



WILEY-
VCH

D53313

ADVANCED FUNCTIONAL MATERIALS



Self-Organized Honeycomb-Microstructured Polystyrene Films

Supramolecular Nanostructuring of Silver Surfaces

Confinement of Thermoresponsive Hydrogels in Porous SiO₂

Soft Lithography of Ceramic Patterns

BICENTENNIAL
1807
WILEY
2007
BICENTENNIAL

DOI: 10.1002/adfm.200600470

A Route to Self-Organized Honeycomb Microstructured Polystyrene Films and Their Chemical Characterization by ToF-SIMS Imaging**

By Sami Yunus,* Arnaud Delcorte, Claude Poleunis, Patrick Bertrand, Alberto Bolognesi, and Chiara Botta

A new type of polymer compound that allows the formation of highly ordered microstructured films by casting from a volatile solvent in the presence of humidity, and its characterization by ToF-SIMS (time-of-flight secondary-ion mass spectrometry) are presented. A honeycomb structure is obtained by activation of 2,2,6,6-tetramethyl-1-piperidinyloxy (TEMPO)-terminated polystyrene (PS) with *p*-toluenesulfonic acid (PTSA). The mechanism of this activation reaction, leading to a more polar PS termination, is deduced from simple experiments and supported by ToF-SIMS characterization. Positive and negative ToF-SIMS imaging allows different chemical regions correlating to the film morphology to be distinguished. This new, straightforward activation process, together with ToF-SIMS chemical imaging, provides a better understanding of the phenomena underlying the formation of these films by directly linking the role of polar terminations to the microscale self-organization. This new method, transposable to other organic acids, suggests interesting new perspectives in the field of self-organized chemical and topographical patterning.

1. Introduction

Self-organization of matter at the micro- and nanoscale is an exciting and promising field of research due to its evident repercussions in many applications (microelectronic, optoelectronic, photonics, sensors, soft lithography)^[1–5] as well as fundamental (thermocapillarity, Bénard–Marangoni instability)^[6] scientific areas. Many spontaneous self-organizing phenomena are currently investigated (dewetting,^[7,8] self-assembly of colloids at an interface,^[9] phase segregation in block copolymers,^[10] etc.). While the latter are now well known and established phenomena, the formation of highly ordered arrays of microcavities, herein concerned, has not yet been fully elucidated.^[11] The reason for this is the complexity of this dynamic phenomenon along with the difficulty to control all the related experimental parameters.

Microstructured films can be formed by the condensation of water microdroplets subsequent to the cooling of the surface

on an evaporating thin layer of polymer solution. After solvent and water evaporation, an imprint of the droplets is left. For the sake of simplicity, this phenomenon, described first by François^[12] and recently covered in a review article by Heiko and Bunz,^[11] is called breath-figure imprinting. Ordering the position and diameter of the cavities in a honeycomb structure requires the tuning of several parameters, such as polymer structure, termination, concentration, solvent, substrate, inert-gas flow, temperature, and humidity.^[13–15] This phenomenon is closely related to Bénard–Marangoni^[16] convection arising in thin layers of a solution submitted to a vertical thermal gradient as claimed by several authors.^[11] Under certain conditions of surface-tension forces, thermal diffusion, and dynamic viscosity, Bénard–Marangoni instability results in a hexagonal pattern of convection spots.^[17] Although ordered breath-figure imprinting is a much more complicated phenomenon, it is strongly dependent on the interfacial forces existing between the water microdroplets and the polymer solution. These forces can be modulated by including polar groups in the polymer that will interact with the water droplets (amphiphilic polymer). Recent experimental work has shown this dependency.^[13–15]

It is of particular interest to use a surface-analysis technique capable of directly imaging the distribution of these end groups on a microstructured film to better understand their role. Some articles have already dealt with surface characterization of such films by using indirect methods.^[18,19] State-of-the-art ToF-SIMS (time-of-flight secondary-ion mass spectrometry) instrumentation provides the chemical composition of the extreme surface (< 3 nm) and includes imaging capabilities on the micrometer scale.^[20] This technique is appropriate to localize the polymer's

[*] Dr. S. Yunus, Prof. A. Delcorte, C. Poleunis, Prof. P. Bertrand
Laboratoire de Physico-Chimie et de Physique des Matériaux
Université Catholique de Louvain
Place Croix du Sud 1, 1348 Louvain-la-Neuve (Belgium)
E-mail: yunus@pcpm.ucl.ac.be

Dr. A. Bolognesi, Dr. C. Botta
Istituto per lo Studio delle Macromolecole
Consiglio Nazionale delle Ricerche
Via E. Bassini 15, 20133 Milano (Italy)

[**] S. Yunus is grateful to the Walloon Region of Belgium for its financial support in the frame of the SENSOTEM research project. A. Bolognesi and C. Botta are grateful to the Miur-Firb RBNE03S7XZ synergy project. The ToF-SIMS equipment has been acquired thanks to the support of the FRFC and the Walloon Region of Belgium.

end-group chemical functions on the self-organized film surface.

In this context, a new family of compounds based on 2,2,6,6-tetramethyl-1-piperidinyloxy (TEMPO) terminated polystyrene is introduced. Although this polymer does not allow breath-figure imprinting, a simple conversion of its termination into an appropriate acid salt triggers this property. This work mainly focuses on the use of *p*-toluenesulfonic acid (PTSA) to do this conversion and the surface chemical characterization of the corresponding ordered films is also shown. Finally, given the relative ease of conversion of 2,2,6,6-tetramethyl-1-piperidinyloxy into the *p*-toluenesulfonate piperidinium (TEMPO/PTS) acid salt, we introduce the possibility of using other organic acids, such as camphorsulfonic acid *R* or *S*, to show the versatility and usefulness of this method in the field of self-organized chemical patterning.

2. Results and Discussion

A number of simple experiments together with ToF-SIMS characterization show that TEMPO-PS reacts with *p*-toluenesulfonic acid in a heterogeneous phase reaction to form a piperidinium salt termination, which allows ordered breath-figure imprinting from a CS₂ solution.

2.1. Breath-Figure Imprinting with PS-TEMPO/PTS

Practically, a carbon disulfide solution of PS-TEMPO on its own does not lead to ordered breath-figure imprinting in our experimental setup. Order is obtained only if a small amount of PTSA is added to this solution and left to react for at least 6 h. Although PTSA seems insoluble in CS₂, in another experiment CS₂ is saturated with PTSA during 48 h, filtered, and then used to prepare a PS-TEMPO solution. This solution does not allow ordered microporous films to be obtained. These simple experiments clearly show an heterogeneous reaction between the TEMPO end groups of polystyrene and PTSA. The most probable reaction is the formation of a *p*-toluenesulfonate piperidinium (TEMPO/PTS) acid salt end group. Figure 1 assesses the high degree of order obtained for films made out of this polymer compound in the presence of humidity.

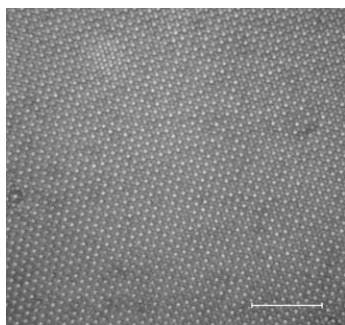


Figure 1. Transmission optical microscopy image of a PS-TEMPO/PTS ordered film (scale bar is 20 μm).

Using carbon disulfide as a solvent and a sufficiently diluted solution usually results in the formation of a monolayer of regular spherical cavities with an average opening-to-cavity diameter ratio of 0.3 to 0.4, as observed from the scanning electron microscopy (SEM) image in Figure 2 and calculated^[21] using Pieranski's model^[22] for colloids at an interface.

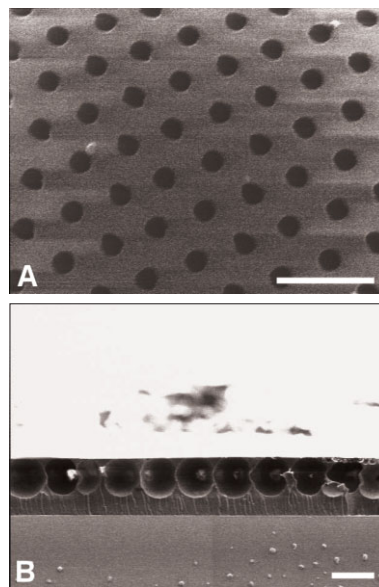


Figure 2. Scanning electron microscopy images of an ordered PS-TEMPO/PTS film (scale bars are 2 μm long). (A) Surface and (B) section of the film.

The high sphericity of the resulting cavities can be better evidenced by molding this type of film with polydimethylsiloxane elastomer (see Fig. 3).^[21,23]

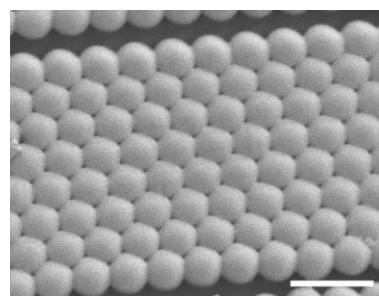


Figure 3. Scanning electron microscopy image of a PDMS film obtained by molding of a PS-TEMPO/PTS film (scale bar is 5 μm long).

2.2. Chemical Characterization of the Microstructured Surfaces

Apart from the high ordering and uniformity of the formed cavities, a chemical patterning is also taking place as a result of the difference in polarity between the polymeric chain and the end groups. Revelation with fluorescent indicators can be used to localize the end groups on the surface of the films. In Figure 4,

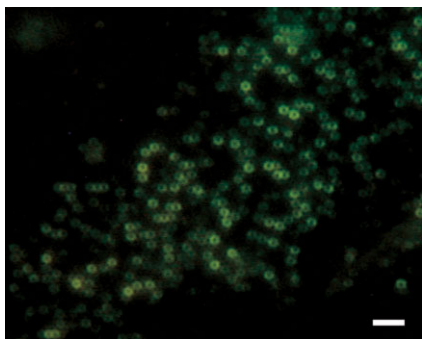


Figure 4. Fluorescence microscopy image of a PS-TEMPO/PTS ordered film sprayed with fluorescein (scale bar is 10 μm long).

fluorescein, whose fluorescence varies upon its acid–basic state, reveals the spherical cavities by fluorescence microscopy, but it does not show the top surface of the film, probably indicating the localization of the end group functions on the surface of the cavities. However, this technique does not allow us to know which component is migrating towards the surface of the cavities: TEMPO, PTSA, or both.

ToF-SIMS was considered to image the surface of the ordered films. As the generated images (256×256 pixels) contain the full mass spectrum at every pixel, it is possible to select images corresponding to atoms or molecular fragments of particular interest. Figure 5 shows a set of SIMS images obtained by summing up the intensities of selected secondary ions.

Figure 5A–C correspond to negative ions; D–F correspond to positive ions. Images A and D show the sum of all secondary ions, B represents the sum of C^- (m/z : 12) and CH^- (m/z : 13), C represents the sum of O^- (m/z : 16), OH^- (m/z : 17), S^- or O_2^- (m/z : 32) and SH^- (m/z : 33)), E represents H^+ (m/z : 1) and F the sum of NH_4^+ (m/z : 18), C_3H_5^+ (m/z : 41), $\text{C}_2\text{H}_4\text{N}^+$ (m/z : 42), $\text{C}_3\text{H}_6\text{N}^+$ (m/z : 56), C_4H_9^+ (m/z : 57), $\text{C}_3\text{H}_8\text{N}^+$ (m/z : 58),

C_5H_9^+ (m/z : 69), $\text{C}_4\text{H}_8\text{N}^+$ (m/z : 70), $\text{C}_3\text{H}_8\text{NO}^+$ (m/z : 74), $\text{C}_8\text{H}_{16}\text{N}^+$ (m/z : 126), $\text{C}_9\text{H}_{18}\text{N}^+$ (m/z : 140), $\text{C}_9\text{H}_{20}\text{N}^+$ (m/z : 142), and $\text{C}_9\text{H}_{20}\text{NO}^+$ (m/z : 158).

Considering the chosen atomic and molecular fragment ions, Figure 5B and E mainly correspond to the polystyrene matrix and the film topographical morphology. Figure 5C mainly represents the PTS composition and Figure 5F relates to the TEMPO composition. As observed in images C and F, the TEMPO and PTS groups are confined on the cavity openings in the form of regular small rings. These geometrical features are very similar to the observations made in Figure 4.

It is also interesting to compare the ToF-SIMS spectra of films obtained in the absence (flat films) and presence of humidity (microstructured films). Figures 6 and 7 show how microstructuring through water condensation strongly enhances the signal peaks correlating to the *p*-toluenesulfonate piperidinium acid salt end groups. Comparison between the negative ToF-SIMS spectra in Figure 6A and B show how the characteristic peaks of the *p*-toluenesulfonate group ($\text{C}_7\text{H}_7\text{SO}_3^-$ and related fragments), displayed in Figure 6C, are strongly enhanced, relatively to the other peaks, when films are ordered through breath-figure imprinting.

The same observation can be made for the characteristic peaks of the piperidinium oxyl group ($\text{C}_9\text{H}_{19}\text{NO}^+$ and related fragments) when comparing the positive ToF-SIMS spectra in Figure 7A and B.

Given the sampling depth of molecular ions in SIMS (ca. 2 nm), these observations demonstrate that the surface of the microstructured samples are strongly enriched with both TEMPO and PTS with respect to flat films.

This semi-quantitative information, obtained from the mass spectra together with the lateral distribution of the chemical functional groups provided by the ToF-SIMS images, confirms that the TEMPO and PTS species preferentially concentrate at the extreme surface of the microcavities during the breath-figure imprinting process.

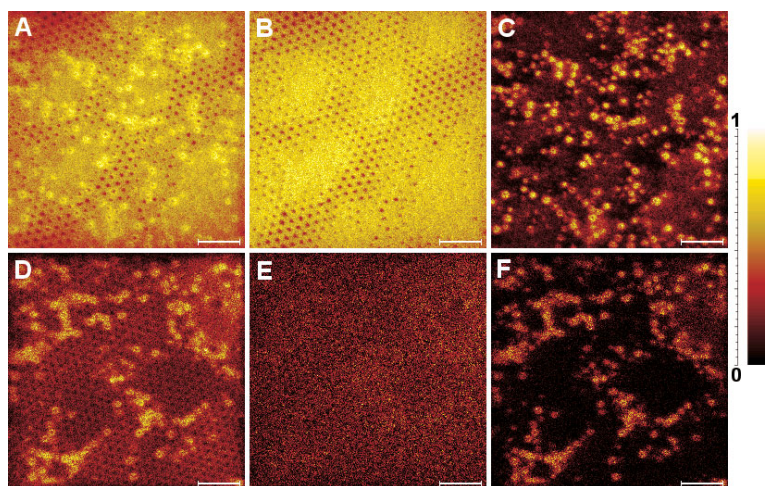


Figure 5. A–C) Negative and D–F) positive ToF-SIMS images (scale bars are 10 μm long). A) Sum of all anions; B) sum of m/z : 12, 13; C) sum of m/z : 16, 17, 32, 33; D) sum of all cations; E) m/z : 1; F) sum of m/z : 18, 41, 42, 56, 57, 58, 69, 70, 74, 126, 140, 142, 158.

2.3. Mechanism of Microstructuring Through Breath-Figure Imprinting

The similarity between the PTS and TEMPO patterns in ToF-SIMS imaging and fluorescence microscopy and the clear signal enhancements in SIMS through breath-figure imprinting strongly suggest that these chemical function interactions are caused by water micelle formation. These interactions, resulting from an acid–basic reaction, exist because of the *p*-toluenesulfonate piperidinium acid salt end group as depicted in Figure 8A. In Figure 8B, these polar end groups, enabling breath-figure imprinting, also allow water micelle formation. Water evaporation leaves empty cavities presenting the polar polymer end groups on their surface.

Assuming the hypothesis of the polymer end group functionalization through salt formation, this auto-organized chemical patterning strategy should not be limited to the use of *p*-toluenesulfonic acid. To

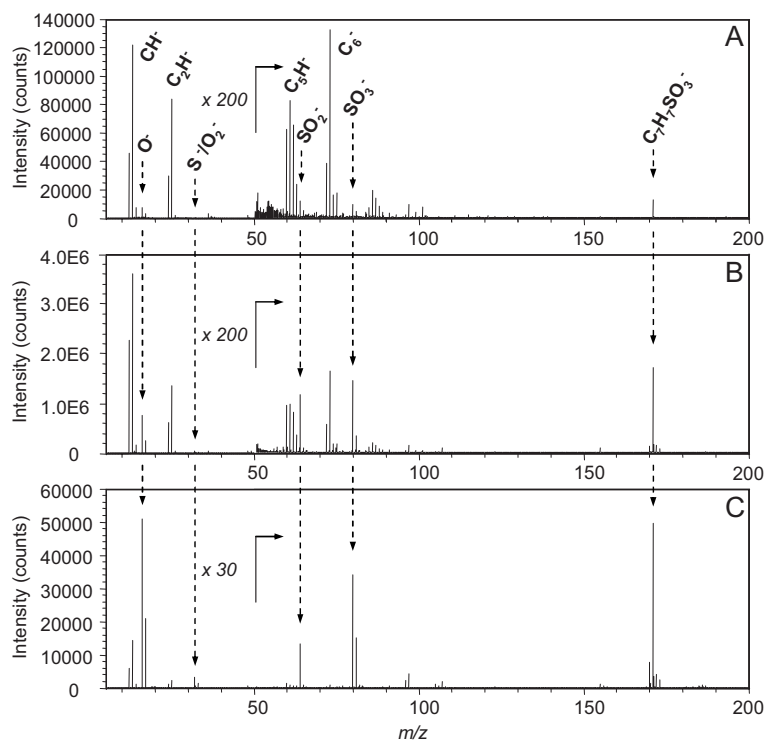


Figure 6. Negative ToF-SIMS spectra of A) a film of PS-TEMPO/PTS obtained in dry nitrogen atmosphere, B) an ordered film of PS-TEMPO/PTS, C) a *p*-toluenesulfonic acid drop-cast film.

further test this hypothesis, ordered films were obtained using exactly the same strategy but with camphorsulfonic acid *R* (CSA(*R*)) instead of PTSA (Fig. 9).

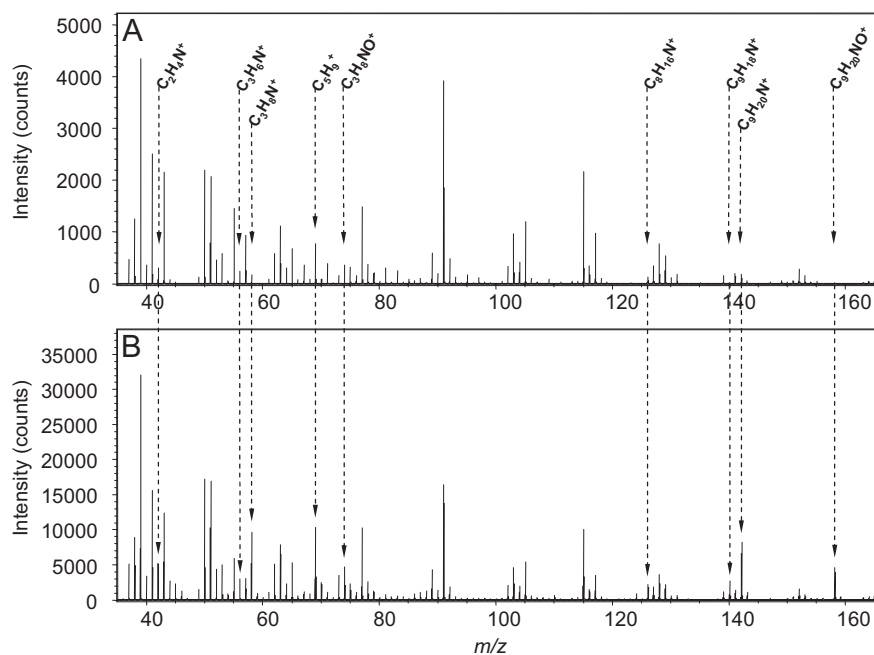


Figure 7. Positive ToF-SIMS spectra of A) a film of PS-TEMPO/PTS obtained in dry atmosphere and B) an ordered film of PS-TEMPO/PTS.

The same observation is valid in this case: ordering of PS-TEMPO is triggered when left to react heterogeneously with a small amount of CSA(*R*) or (*S*) in CS₂ for some time. From a structural viewpoint, the films obtained with CSA seem less ordered and have smaller cavities when compared to ordered films obtained with PTSA. Nevertheless, this additional result supports our proposed mechanism of microstructuring.

3. Conclusions and Perspectives

This work shows how PS-TEMPO, a polymer which is commonly used nowadays, can easily be functionalized to prepare ordered honeycomb microstructured films by breath-figure imprinting. This property is triggered by conversion of its piperidinyloxy end group into a *p*-toluenesulfonate or camphorsulfonate acid salt. The increased polarity of this new end group is believed to allow ordered breath-figure imprinting through water micelle formation and Bénard–Marangoni convection enhancement. Considering that Bénard–Marangoni convection is responsible for ordering,^[11,17] PS-TEMPO constitutes a model compound in this field: its end group interconversion into an acid salt is easy and PS-TEMPO alone does not allow ordered breath-figure imprinting. Using this polymer and different organic acids

could allow a statistical study of the order, size, and opening-to-diameter ratio of the cavities to better understand ordered breath-figure imprinting. This was already confirmed with the camphorsulfonic *R* acid as proof. As an example, the opening-to-cavity diameter ratio determined by SEM images of ordered film cross sections could be related to the interfacial tension between the polymer/CS₂ solution and water.^[21]

A surface organization through water micelle formation has commonly been considered and is well accepted for polymer end groups when present. Some articles have already dealt with the surface characterization of such films by using indirect methods.^[18,19] In the present work, polymer end-group migration is directly observed by ToF-SIMS imaging and confirmed by comparison of spectra of flat and ordered films. The results obtained in the case of PS-TEMPO are transposable to other polymers allowing ordered breath-figure imprinting. In this context, ToF-SIMS characterization seems well adapted to this field and should be applied to the long list of polymer compounds already reported in the literature for these applications.^[11–13,24–27]

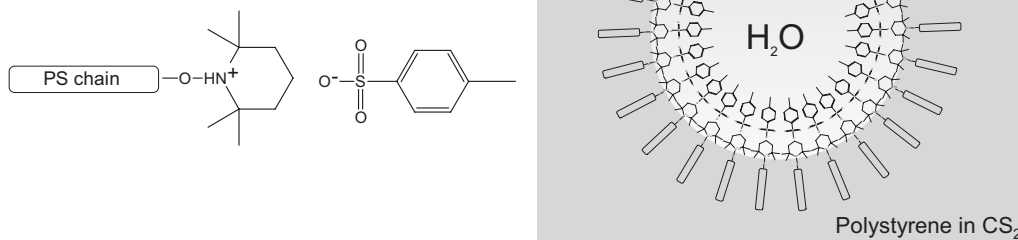


Figure 8. A) Molecular structure of *p*-toluenesulfonate piperidinium end group and B) schematic representation of its arrangement in micelles during film formation.

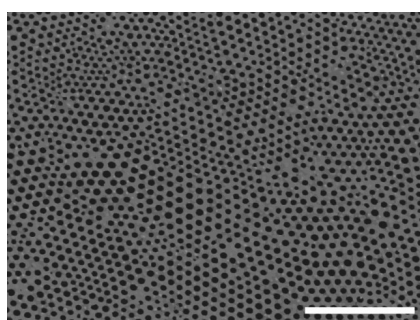


Figure 9. Scanning electron microscopy image of a PS-TEMPO/CSA (R) ordered film (scale bar is 10 μm).

This work has conclusively shown that ordering is not only topographical but chemical as well, raising interesting perspectives in the field of chemical patterning (i.e., self-assembled chemically functionalized picoscale beakers).

4. Experimental

Sample Preparation: PS-TEMPO (weight-average molecular weight $M_w = 6500$, polydispersity $M_w/M_n = 1.5$) was obtained by controlled free radical polymerization of styrene using 2,2,6,6-tetramethyl-1-piperidinyloxy (TEMPO) [28]. The solution of PS-TEMPO was prepared in HPLC grade carbon disulfide (0.6%) and a small amount of PTSA (*p*-toluenesulfonic acid) was added and allowed to react for at least six hours. This solution was then filtered with a nylon syringe filter (0.45 μm). Ordered holey films were obtained by evaporating a drop of the solution under a humid atmosphere on 10 mm \times 10 mm pieces of silicon wafer or 15 mm \times 15 mm microscope cover slides. The humid atmosphere was generated by flowing nitrogen through water at ambient temperature using a sintered glass bubbler. The moisturized nitrogen flux was directed towards the polymer solution surface using appropriate tubing. For ToF-SIMS analysis purposes, flat films were obtained in the same way but without humidity.

Fluorescent films were obtained by exposing the PS-TEMPO/PTS ordered films to an ultrasonic spray of a fluorescein sodium salt aqueous solution (2 %).

The beaded PDMS films (negative imprints [29]) were obtained by pouring a degassed mixture of PDMS prepolymer and curing agent (Dow Corning, Sylgard 184) directly on the PS holey films and placing these preparations in an oven at 80 $^{\circ}\text{C}$ for 4 h. The beaded PDMS films were then released from the PS films by placing them in hot dichloromethane.

Imaging and Measurements: ToF-SIMS spectra and images were recorded on a PHI-Evans TFS-4000 MMI (TRIFT) spectrometer. For images, the samples were bombarded with a pulsed $^{69}\text{Ga}^+$ ion beam (25 keV, 600 pA d.c., 14.5 kHz frequency, and 17.7 ns pulse width). The analyzed area was a square of 60 $\mu\text{m} \times 60 \mu\text{m}$. With a 30 min data acquisition time, the fluence was about 4×10^{13} ions cm^{-2} , which is close to static conditions. The spectra in Figures 7B and 8B were extracted from ToF-SIMS image measurements displayed in Figure 5. For the spectral measurements, samples were bombarded with a pulsed $^{69}\text{Ga}^+$ ion beam (15 keV, 1.2 nA d.c., 8.2 kHz frequency, and 22 ns pulse width). The analyzed area was a square of 121 $\mu\text{m} \times 121 \mu\text{m}$. With a 5 min data acquisition time, the fluence was about 2.8×10^{12} ions cm^{-2} , which ensured static conditions. In both cases, the secondary ions were accelerated to a kinetic energy of ± 3 keV by applying a bias on the sample. In order to increase the detection efficiency of high mass ions, a 7 kV post-acceleration voltage was applied at the detector entry.

Optical microscopy images were obtained in air with a Leitz Dialux 20 equipped with a Ploemopak fluorescence vertical illuminator with three filter positions and a digital camera. For fluorescence imaging, a 450–490 nm band-pass excitation filter was used.

Scanning electron microscopy images were recorded using a Zeiss Leo 982 apparatus.

Received: May 30, 2006

Revised: October 3, 2006

Published online: March 2, 2007

- [1] C. De Rosa, C. Park, E. L. Thomas, B. Lotz, *Nature* **2000**, *405*, 433.
- [2] D. Zhao, J. Feng, Q. Huo, N. Melosh, G. H. Fredrickson, B. F. Chmelka, G. D. Stucky, *Science* **1998**, *279*, 548.
- [3] B. Erdogan, L. Song, J. N. Wilson, J. O. Park, M. Srinivasarao, U. H. F. Bunz, *J. Am. Chem. Soc.* **2004**, *126*, 3678.
- [4] A. Bolognesi, C. Botta, S. Yunus, *Thin Solid Films* **2005**, *492*, 307.
- [5] S. Yunus, F. Spano, A. Bolognesi, C. Botta, G. Patrinoiu, D. Brühwiler, A. Z. Ruiz, G. Calzaferri, *Adv. Funct. Mater.* **2006**, *16*, 2213.
- [6] M. Li, S. Xu, E. Kumacheva, *Langmuir* **2000**, *16*, 7275.
- [7] E. Schäffer, T. Thurn-Albrecht, T. P. Russel, U. Steiner, *Nature* **2000**, *403*, 874.
- [8] A. M. Higgins, R. A. Jones, *Nature* **2000**, *404*, 476.
- [9] L. E. Helseth, T. M. Fischer, *Phys. Rev. E* **2003**, *68*, 051403.
- [10] G. Krausch, R. Magerle, *Adv. Mater.* **2002**, *14*, 1579.
- [11] U. Heiko, F. Bunz, *Adv. Mater.* **2006**, *18*, 973.
- [12] M. Srinivasarao, D. Collings, A. Philips, S. Patel, *Science* **2001**, *292*, 79.
- [13] V. Govor, I. A. Bashmakov, R. Kiebooms, V. Dyakonov, J. Parisi, *Adv. Mater.* **2001**, *13*, 588.
- [14] O. Pitois, B. François, *Eur. Phys. J. B* **1999**, *8*, 225.
- [15] R. F. Probstein, *Physicochemical Hydrodynamics: An Introduction*, Butterworth, Boston, MA **1989**.
- [16] S. Xu, M. Li, Z. Mitov, E. Kumacheva, *Prog. Org. Coat.* **2003**, *48*, 227.
- [17] M. H. Stenzel, T. P. Davis, *Aust. J. Chem.* **2003**, *56*, 1035.

- [18] H. Yabu, M. Shimomura, *Langmuir* **2006**, *22*, 4992.
- [19] P. Bertrand, L. T. Weng, *Mikrochim. Acta* **1996**, *13*, 167.
- [20] A. Bolognesi, M. Civardi, D. Comoretto, C. Mercogliano, A. Turturro, S. Yunus, *Langmuir* **2005**, *21*, 3480.
- [21] P. Pieranski, *Phys. Rev. Lett.* **1980**, *45*, 569.
- [22] H. Yabu, M. Shimomura, *Langmuir* **2005**, *21*, 1709.
- [23] B. François, G. Widawski, M. Rawiso, B. Cesar, *Synth. Met.* **1995**, *69*, 463.
- [24] B. De Boer, U. Stalmach, H. Nijland, G. Hadziioannou, *Adv. Mater.* **2000**, *12*, 1581.
- [25] V. Govor, I. A. Bashmakov, F. N. Kaputski, M. Pientka, J. Parisi, *Macromol. Chem. Phys.* **2000**, *201*, 2721.
- [26] J. Peng, Y. Han, J. Fu, Y. Yang, B. Li, *Macromol. Chem. Phys.* **2003**, *204*, 125.
- [27] T. Hayakawa, S. Horiuchi, *Angew. Chem. Int. Ed.* **2003**, *42*, 2285.
- [28] S. Kobatake, H. J. Harwood, R. P. Quirk, D. B. Priddy, *J. Polym. Sci. A: Polym. Chem.* **1998**, *36*, 2555.
- [29] G. M. Whitesides, Y. Xia, *Angew. Chem. Int. Ed.* **1998**, *37*, 550.
-